Steady-state supercritical CO2 and brine relative permeability measurements at different pressure conditions

Bo Gao[1], *Elizabeth* Lyons[2], *Daulet* Magzymov[2], *Larry* Poore[3], *Gloria* Besil[2], *Stacy* Richardson[2,*], *Lisa* Lun[2]

[1]ExxonMobil Upstream Company, Spring, TX, USA
[2]ExxonMobil Technology & Engineering Company, Spring, TX, USA
[3]Contractor to ExxonMobil (formerly ExxonMobil Technology & Engineering Company, Spring, TX, USA)

Abstract. Relative permeability is one of the most important properties influencing the transport of CO_2 in the subsurface. While increasing amount of experimental work has been published in recent years, the reported data often provide contradictory conclusions regarding supercritical CO_2 and brine ($scCO_2$-brine) flow behavior. Some past work suggests such system is sensitive to variations in reservoir conditions, through the influence of evolving fluid-rock properties, in particular wetting characteristics. In this study, we intentionally design an experimental program to focus on the impact of reservoir pressure on the relative permeability of the $scCO_2$-brine system. Pore pressure has been varied across a much wider range than most literature (77°C [170°F], 12.4 to 30 MPa [1800 to 4350 psi]), representative of conditions under which conflicting contact angle data have previously been reported. We measure both drainage and imbibition relative permeabilities using the steady-state method on a single Berea sandstone core. ExxonMobil's SCAL expertise and best practices have been fully leveraged in designing and executing the experimental program. Significant system and procedural upgrades are implemented to overcome operational challenges commonly associated with the $scCO_2$-brine system, and thus enabling high quality data collection. The results from this study help develop high confidence recommendations regarding the role of pressures, hence wetting conditions, on the $scCO_2$-brine relative permeability behaviors. The operational aspects reported here contribute to the development of best practices for making relative permeability measurements for CO_2 storage projects.

1 Background

Predictive modeling of CO_2 geological storage is a key requirement of emerging storage standards and regulations. For storage in deep saline formations, where CO_2 is injected into the pore spaces of rocks previously occupied by brine, relative permeability is an important input parameter for predictive models. The plethora of literature in recent years has not painted a harmonized picture of supercritical CO_2 ($scCO_2$) and brine relative permeability behavior in the storage setting. Some research studies suggest sensitivity to variations in reservoir conditions (e.g., pressure), through the influence of evolving fluid-rock interactions, in particular wetting characteristics through contact angle measurements [1-10]. Such claims will have significant impact on the fate of CO_2 geological storage [11-18], both in terms of CO_2 plume movement, as well as structural and residual CO_2 trapping mechanisms.

ExxonMobil has devised a multi-pronged approach to investigate the behavior of the rock and fluid interaction of $scCO_2$ and brine in the subsurface [19-23], through collaboration with external research organizations, as well as building our internal experimental capabilities. CO_2 geological storage is a growing business, and as such, we desire to confidently conduct $scCO_2$-brine relative permeability experiments at geological storage conditions. We also desire to understand wettability as some papers [1-10] claim contact angle / wettability evolution. Therefore, we set out to directly examine how wettability is manifest through relative permeability relationships. In parallel to this study, we are making advances on direct and high-quality measurements of contact angle from collaboration with NETL [20]. Through these efforts, we hope to contribute to the existing dataset for $scCO_2$-brine systems.

Direct comparison of relative permeability curves under different geological storage conditions, to our knowledge, has not been reported before. This study presents a unique experimental design that focuses on the impact of reservoir pressure on the relative permeability of the $scCO_2$-brine system. The results obtained in this study contributes a set of relative permeability curves for $scCO_2$-brine measured under conditions free from mass transfer between $scCO_2$ and brine.

2 Materials and Methods

A Clear Birmingham Buff Berea sandstone long core sourced from Cleveland Quarries was used for the studies. The core was 3.81 cm in diameter and 30.7 cm in length and had a 16.5% porosity and absolute gas permeability 51.8 mD.

The core was cleaned with a series of solvents and dried before use to ensure the core was fully cleaned and in a water-wet condition. The core was then saturated with synthetic

* Corresponding author: stacy.l.richardson@exxonmobil.com

brine. To achieve a 100% liquid saturation in the core, first a vacuum is pulled, and dead brine is metered in until the targeted pressure is achieved. The metered dead brine represents one pore volume and was confirmed against the helium-based pore volume. Once installed in the test system, the live brine is injected to displace the dead brine. A brine formulation of 4 wt% NaCl was used in all experiments to: a) alleviate chemical incompatibility if using a more complex formulation; b) achieve a total salinity of 40 kppm; c) minimize salt precipitation after vacuum distillation to ensure the quality of material balance. The salinity was based on a water analysis from a legacy ExxonMobil US Gulf of Mexico asset.

The experimental program was intentionally designed to focus on the impact of reservoir pressure on the relative permeability of the $scCO_2$-brine system. Pore pressure was varied across a much wider range than most literature (77°C [170°F], 12.4 to 30 MPa [1800 to 4350 psi]), representative of conditions under which conflicting contact angle data was previously reported. The differential pressure across the core was controlled to minimize potential fluid mass transfer / mutual solubility changes in the system. The net confining stress used was 17.4 MPa (2525 psi). The core was installed in a vertical position and flow was injected from the top and produced from the bottom.

The testing apparatus was adapted and modified from the recirculating steady-state relative permeability measurement system design (Figure 1) [24]. High precision Quizix fluid pumps, acting in pairs, were used to deliver $scCO_2$ and brine. A third gas pump was used to maintain system pressure. The New England Research Inc. acoustic separator allowed for complete system recirculation. Pressure drop across the core was measured using upstream and downstream ParoScientific absolute pressure transducers.

Saturation quantification was derived through tracking the fluid level in the acoustic separator. In-situ saturation monitoring (ISSM) was not employed. Therefore, average saturations inside the core, rather than saturation profiles, were measured during testing. In our experience, saturation quantification from acoustic separator has been proven to be of high accuracy when tests are performed in a recirculating system using the steady-state method. While ISSM has the benefit of additional data collection, it adds additional complexity to experimental execution and should be calibrated by other independent methods, such as acoustic separator levels and post-test material balance checks.

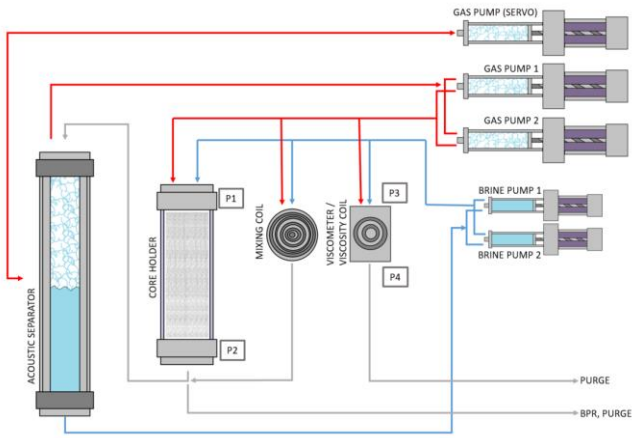

Fig. 1. Schematic of steady-state relative permeability system.

The test was first performed at a pore pressure of 12.4 MPa (1800 psi) with equilibrated fluids, and then repeated at a higher pore pressure of 30 MPa (4350 psi), using the steady-state method. After the first test cycle at 12.4 MPa (1800 psi), the system pressure was increased through gradual pressure steps to 30 MPa (4350 psi) while maintaining the NCS at 17.4 MPa (2525 psi). As the system pressure was being raised, the fluids were continuously being recirculated through the mixing coil. At the higher pressure of 30 MPa (4350 psi), the $scCO_2$ and brine reached a new equilibrium.

The $scCO_2$-brine relative permeability tests at each pressure included the following major steps: live absolute brine permeability, $scCO_2$-brine primary drainage cycle (increasing $scCO_2$ fractional flows to model $scCO_2$ displacing live brine during $scCO_2$ injection), $scCO_2$-brine primary imbibition cycle (increasing brine fractional flows to model live brine displacing and trapping $scCO_2$ during post injection), and $scCO_2$-brine secondary drainage cycle.

Flow tests at each pressure were followed by depressurization, vacuum distillation, and solvent extraction to clean the core and quantify final fluid saturation as a critical check for overall material balance. Finally, the core was dried, and post-test gas permeability and pore volume were measured.

Experimental conditions and fluid properties are summarized below in Table 1. The Kestin correlation [25] was utilized for the brine viscosity, and the National Institute of Standards and Technology (NIST) [26] was used for the $scCO_2$ viscosity.

Table 1: Fluid properties under testing conditions

	Lower Press. 12.4 MPa (1800 psi) 77 °C (170 °F)	**Higher Press. 30 MPa (4350 psi) 77 °C (170 °F)**
Visc. Brine [cP]	0.405	0.410
Visc. CO_2 [cP]	0.026	0.066
Viscosity Ratio, Brine/CO_2	15.6	6.21

Table 2 summarizes dimensions and basic properties of the Berea long core used both 12.4 MPa (1800 psi) and 30 MPa (4350 psi) tests.

Table 2: Berea long core properties

Length [cm]	30.7
Diameter [cm]	3.81
Porosity [%]	16.5
Absolute Gas Perm., Pre-test [mD]	51.8
Absolute Gas Perm., Post-test (12.4 MPa) [mD]	54.9
Absolute Gas Perm., Post-test (30 MPa) [mD]	52.9
Absolute Brine Perm,. (12.4 MPa) [mD]	33.4
Absolute Brine Perm,. (30 MPa) [mD]	29.8

3 Results

The detailed experimental data, including total flow rate (Qt), pressure drop across the core (dP), fractional flow (Fw), average brine saturation (Sw), and calculated relative permeability (Krg and Krw) for both 12.4 MPa (1800 psi) and 30 MPa (4350 psi) tests, are included below in Table 3 and Table 4.

Table 3: Relative permeability of the $scCO_2$-brine system for primary drainage, primary imbibition, and secondary drainage at 12.4 MPa (1800 psi)

Fw [frac]	Qt, [cc/min]	dP [psi]	Sw [frac PV]	Krg, [frac Kw]	Krw [frac Kw]
Primary drainage					
1	2.0	15.9	1	0	1
0.909	2.0	20.3	0.933	0.005	0.716
0.745	2.0	21.8	0.886	0.012	0.546
0.500	3.0	31.8	0.849	0.024	0.376
0.262	2.5	18.7	0.812	0.051	0.280
0.070	5.0	20.5	0.723	0.117	0.135
0.009	6.0	12.4	0.588	0.247	0.034
0.0001	6.0	6.7	0.427	0.463	0.001
0	8.0	8.1	0.417	0.508	0
0	12.0	11.1	0.417	0.557	0
0	16.0	14.1	0.402	0.586	0
Primary imbibition					
0	8.6	7.7	0.405	0.577	0.001
0.009	6.0	21.3	0.598	0.144	0.020
0.070	1.5	25.8	0.630	0.028	0.032
0.262	0.5	28.8	0.638	0.007	0.036
0.745	0.2	30.7	0.649	0.001	0.039
0.908	0.05	10.5	0.644	0.0002	0.035
1	0.05	11.2	0.648	0	0.035
Secondary drainage					
0.262	0.5	26.9	0.655	0.007	0.039
0.009	4.0	15.4	0.610	0.133	0.018
0.005	4.0	13.2	0.594	0.155	0.012

Table 4: Relative permeability of the $scCO_2$-brine system for primary drainage at 30 MPa (4350 psi)

Fw [frac]	Qt, [cc/min]	dP [psi]	Sw [frac PV]	Krg [frac Kw]	Krw [frac Kw]
Primary drainage					
1	2.0	18.1	1	0	1
0.916	1.5	17.7	0.925	0.010	0.702
0.898	1.5	17.8	0.921	0.013	0.686
0.686	1.5	18.4	0.869	0.038	0.507
0.472	1.5	16.7	0.832	0.070	0.384
0.194	2.0	17.0	0.751	0.139	0.207
0.054	2.5	13.3	0.651	0.262	0.093
0.018	4.0	15.7	0.579	0.367	0.040
0.004	6.0	16.9	0.505	0.520	0.013
0	8.0	16.1	0.410	0.727	0
0	12.0	23.5	0.390	0.749	0
0	16.0	29.8	0.353	0.788	0

For successful steady-state relative permeability tests, it is critically important to ensure steady-state is reached through real-time monitoring of pressure drop across the core and separator fluid level for an extended period at each fractional flow. Depending on fractional flow, steady-state is typically reached from a few hours to a few days. During the test, the pressure drop and separator level along with other live data streams, such as pump volumes and fluid velocities, were monitored in real time. The determination of steady-state and timing to move onto the next fractional flow stage were based on comparing pre-test design vs. actual lab observation and joint decision by the SCAL engineer and lab professional.

A complete test history of pressure drop and acoustic separator level for primary drainage at 12.4 MPa (1800 psi) is presented in Figure 2, to showcase the high-quality raw lab data used to generate the relative permeability curves.

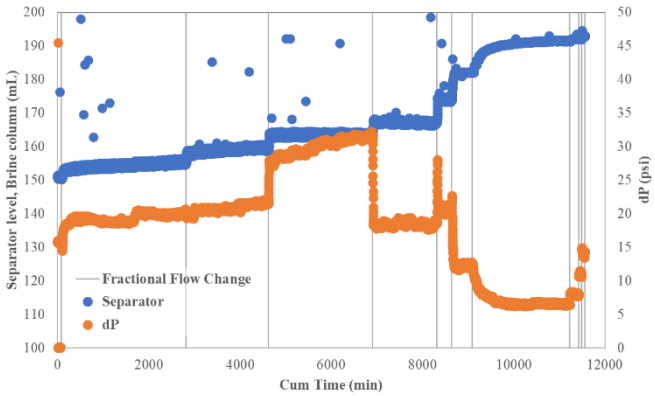

Fig. 2. Raw lab pressure drop and acoustic separator level as a function of test time, for primary drainage at 12.4 MPa (1800 psi)

3.1 Comparison of $scCO_2$-brine primary drainage relative permeability at 12.4 Mpa (1800 psi) vs. 30 Mpa (4350 psi)

The $scCO_2$-brine primary drainage relative permeability curves describe the process of injecting $scCO_2$ into underground saline aquifer. As mentioned in the introduction, the primary objective of current experimental program is to investigate impact of pressure on $scCO_2$-brine relative permeability behavior.

As shown in Figure 3, primary drainage relative permeability curves from 12.4 MPa (1800 psi) and 30 MPa (4350 psi) are plotted together. Absolute brine permeability (Kw) measured at the beginning of the test was used as reference to calculate relative permeability. The measured Kw were 33.4 mD at 12.4 MPa (1800 psi) and 29.8 mD at 30 MPa (4350 psi) using the viscosity values listed in Table 1.

It is worth noting the absolute brine permeabilities are ~60% of the absolute gas permeability, 51.8mD. In our experience it is not uncommon to observe absolute brine permeability values less than absolute gas permeability. When using a reservoir simulator to model the storage of $scCO_2$ in saline aquifers, it is necessary to ensure that appropriate transforms are used to link the permeability data type used to build the geologic model (e.g., absolute gas permeability) to the reference permeability of the relative permeability functions (e.g., absolute brine permeability); as evidenced above, this transform can be significant, ~60%.

The relative permeability curves between the two pressures were similar. The difference in relative permeability curves between the two pressures was not significant, as evidenced by the comparison shown in Figure 3. Towards the end of the test at lower water saturation, there was evidence of capillary end effect which could contribute to the observed difference. The error whiskers in Figure 3 reflect the uncertainty in saturation quantification of the system of +/- 0.02 saturation fraction. Our observation of minimal effect of pressure on relative permeability is consistent with other ongoing research efforts in understanding wettability evolution under CO_2 storage conditions [20].

The water saturation at the end of the steady-state relative permeability drainage test is still higher than true irreducible water saturation. To better define irreducible water saturation, we recommend experimental techniques like multi-speed centrifuge and/or porous plate should be employed, though true reservoir/storage condition capillary pressure tests continue to be a challenge to execute in the lab.

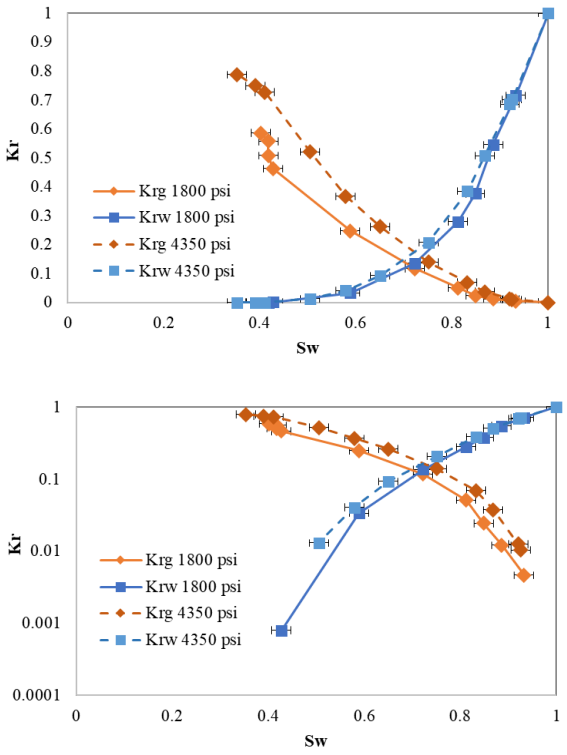

Fig. 3. Relative permeability of the $scCO_2$-brine system for primary drainage at 12.4 MPa (1800 psi) and 30 MPa (4350 psi) pore pressure: a. linear plot, b. semi-log plot.

Best practices were leveraged to mitigate capillary end effects. These include the use of the steady-state recirculating system [24], the use of long core and high flow rates (to the extent possible) [27], and multi-rate testing including bump rates at the end of drainage / imbibition test cycles [28]. Bump rates at the end of 100% $scCO_2$ injection were implemented to correct for capillary end effects. The test design was informed from prior similar tests using a multi-rate scheme following the analytical Intercept Method [28] which observed minimal end effect with the rate design implemented. Therefore, coreflood simulation was not utilized for data analysis due to our experience with the analytical Intercept Method and its application towards a robust test design.

3.2 Hysteresis behavior in $scCO_2$-brine relative permeability curves at 12.4 MPa (1800 psi)

The $scCO_2$-brine primary imbibition relative permeability curves describe the process of brine displacing $scCO_2$ plume during the post-injection period, and therefore have direct impact on CO_2 long term storage. At the time of writing this paper, imbibition relative permeability tests at the higher pressure are still ongoing. Therefore, the imbibition data at 30 MPa (4350 psi) is not reported. Figure 4 shows both primary drainage and the subsequent primary imbibition relative permeability cycles from the lower pressure 12.4 MPa (1800 psi) tests. Negligible hysteresis is observed in the brine phase relative permeability curves, which is consistent with the expectations for the wetting phase in a gas-liquid system with strong wetting and non-wetting phase behavior. However,

significant hysteresis is observed in the gas ($scCO_2$) phase relative permeability curves, due to trapped gas saturation during the imbibition process. As a result, drainage and imbibition curves follow the expected strongly water-wet displacement behavior. The Land correlation [29] can be used to describe the relationship between the observed trapped gas and initial gas (endpoint of the drainage curve/starting point of the imbibition curve) saturations. Note that because the drainage curve did not reach the true irreducible water saturation, the imbibition curve represents a scanning curve rather than a true bounding imbibition curve [30]; the bounding trapped gas saturation is expected to be higher than the observed trapped gas saturation.

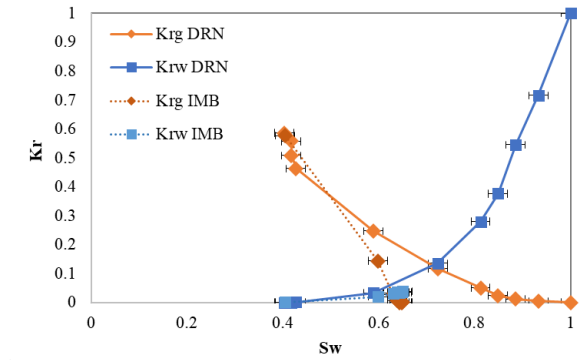

a.

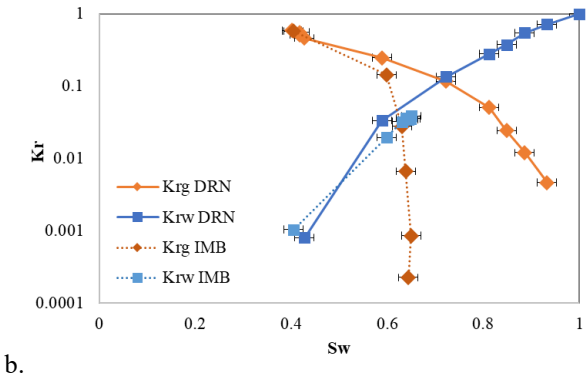

b.

Fig. 4. Relative permeability of the $scCO_2$-brine system for primary drainage and primary imbibition at 12.4 MPa (1800 psi): a. linear plot, b. semi-log plot.

In addition to the primary drainage and primary imbibition cycles, we also performed an abbreviated secondary drainage cycle to understand hysteresis behavior of additional saturation reversal that could potentially take place in more complicated storage settings. The resulting curves from secondary drainage cycle are shown in Figure 5. Secondary drainage hysteresis behavior was not observed for the Berea sample at 12.4 MPa (1800 psi). This could potentially help simplify input requirements for modeling and simulating such processes in subsurface studies.

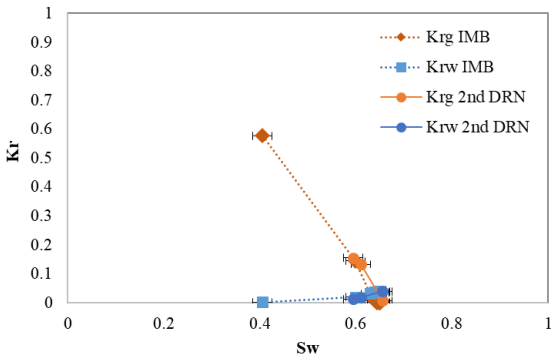

a.

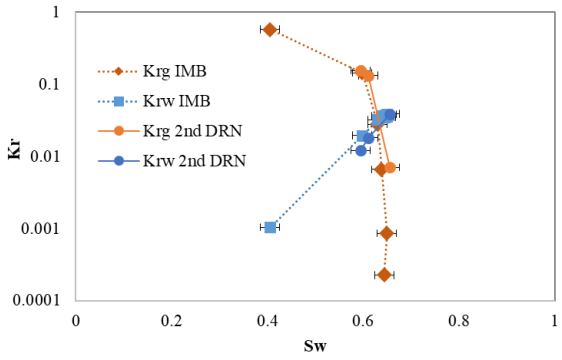

b.

Fig. 5. Relative permeability of the $scCO_2$-brine system for primary imbibition and secondary drainage at 12.4 MPa (1800 psi): a. linear plot, b. semi-log plot.

3.3 Practical recommendations

Among many experimental attempts to measure $scCO_2$-brine relative permeability, we observe key differences in sample preparation, fluid equilibration procedures, experimental techniques, and test conditions. Significant system and procedural upgrades are implemented in our lab testing program to overcome operational challenges commonly associated with the $scCO_2$-brine system, and thus enabling high quality data collection. To overcome the risk of potential failure of O-rings during the test we used specialized AFLAS® elastomer material in seals that come in contact with $scCO_2$ and brine. Moreover, all wetted components of the system were upgraded to Hastelloy C to avoid potential corrosion risks due to presence of CO_2, brine, and elevated temperatures. The test design incorporated long core, high flow rates and bump rates to mitigate capillary end effects, as described in Section 3.1. Lastly, we closely monitored the real-time data streams and allowed time to achieve steady-state at each fractional flow.

Relative permeability concept applies to immiscible fluids or fluids that are at equilibrium. Dead brine and purified $scCO_2$ are partially miscible, meaning $scCO_2$ dissolves in brine and water evaporates into the $scCO_2$ phase [31]. This mass transfer has a critical impact on quantification of saturation values to construct relative permeability curves. For example, continuous injection of unequilibrated CO_2 into dead brine core would ultimately result in complete evaporation of water in the core, resulting in near zero irreducible water saturation ($S_{wirr} = 0$). Similarly, injection of fresh brine in unequilibrated $scCO_2$ filled core will ultimately

result in near zero trapped gas saturation (S_{gt} = 0), because $scCO_2$ will dissolve in fresh dead brine. Therefore, relative permeability measurements with unequilibrated fluids are not reliable to estimate multiphase displacement behavior.

To achieve fluid equilibrium, we upgraded fluid preparation and system charging procedures. To prepare the brine for our tests, 4 wt% NaCl solution and high purity CO_2 were charged into a piston cell with 5.5 MPa (800 psig) head pressure and rocked to engage the mixing ring in the cell. This process was repeated until the pressure stabilized. Next the piston cell was placed in the system oven and heated to test temperature (77°C [170°F]). The piston cell was rocked again several times at temperature. Once stable, the excess gas cap of CO_2 was bled from the top sample side. To ensure fluid equilibrium, the pre-livened brine and the CO_2 were circulated through the system's mixing coil. The fluids were recirculated until system stability was reached. This step was time consuming which took several weeks for our system volume, but a key factor for a successful test.

The $scCO_2$-brine system is sensitive to pressure and temperature fluctuations. Relative permeability tests are conducted at isothermal conditions while pressure varies during the test. Controlling the differential pressure across the core promotes stable acoustic separator levels for saturation quantification. For these tests on the Berea long core, we found a differential pressure below 0.2 MPa (30 psi) was suitable for most fractional flows. Such pressure differential constraints impose limits on maximum flowrate that can be applied across the core.

The recirculating steady-state system allows for continuous fluid equilibrium throughout the test cycles. Other systems, such as non-recirculating steady-state and unsteady-state, are challenged as externally equilibrated fluids will be sensitive to temperature and pressure variations and may not maintain a true fluid equilibrium. Therefore, we recommend utilizing recirculating steady-state systems with equilibrated fluids at pressure and temperature for the $scCO_2$-brine relative permeability tests.

4 Conclusions

In this paper, we have presented the comparison of steady-state relative permeability curves for the $scCO_2$-brine system at pore pressures much higher than most literature (77°C [170°F], 12.4 to 30 MPa [1800 to 4350 psi]). We did not observe significant difference in relative permeability behavior between the two pore pressures during drainage cycles. This observation is consistent with other ongoing research efforts coordinated through our CO_2 storage technology portfolio [20]. We also presented drainage and imbibition curves at 12.4 MPa (1800 psi) to understand primary imbibition hysteresis behavior and trapped $scCO_2$ saturation. The drainage and imbibition curves follow the expected strongly water-wet displacement behavior. The lack of significant hysteresis during secondary drainage cycle presents opportunity to simplify simulation workflow should such processes becomes relevant in CO_2 storage setting.

This work has found no pressure effects on $scCO_2$-brine relative permeability; no wettability effects are inferred.

At this time, we recommend conducting relative permeability experiments at reservoir/storage condition to expand experience and dataset for $scCO_2$ storage applications. Further, research efforts are under way to modify the established capillary pressure measurement techniques to enable reservoir conditions experiments and hence describe the fluid flow properties toward irreducible water saturation.

ExxonMobil Technology & Engineering Company is acknowledged for giving permission to publish this work. A special thanks to Chick Wattenbarger, Jon Meissner, Zhidong Li, Alana Leahy-Dios, Jennifer Rainey, and Andrew Heider for valuable discussions and comments to the manuscript.

References

1. P. Chiquet, D. Broseta, S. Thibeau, Wettability alteration of caprock minerals by carbon dioxide, Geofluids, 7, 112-122 (2007)
2. Y. Sutjiadi-Sia, P. Jaeger, R. Eggers, Interfacial phenomena of aqueous systems in dense carbon dioxide, J. Supercritical Fluids, 46(3), 272-279 (2008)
3. PK Bikkina, Contact angle measurements of CO2–water–quartz/calcite systems in the perspective of carbon sequestration, Int. J. Greenh. Gas Control, 5(5), 1259-1271 (2011)
4. J. Mills, M. Riazi, M. Sohrabi, Wettability of common rock-forming minerals in a CO2-brine system at reservoir conditions, SCA2011-06 presented at the International Symposium of the Society of Core Analysts, Austin, USA, 18-21 September 2011
5. R. Farokhpoor, BJA Bjorkvik, E. Lindeberg, O. Torsater, CO2 Wettability Behavior During CO2 Sequestration in Saline Aquifer -An Experimental Study on Minerals Representing Sandstone and Carbonate, Eng. Procedia, 37, 5339-5351 (2013)
6. S. Iglauer, CH Pentland, A. Busch, CO2 wettability of seal and reservoir rocks and the implications for carbon geo-sequestration, Water Resour. Res., 51, 729-774 (2014)
7. M. Arif, A. Al-Yaseri, A. Barifcani, M. Lebedev, S. Iglauer, Impact of pressure and temperature on CO2-brine-mica contact angles and CO2-brine interfacial tension: Implications for carbon geo-sequestration, J. Coll. Interf. Sci., 462, 208-215 (2016)
8. S. Iglauer, CO2–Water–Rock Wettability: Variability, Influencing Factors, and Implications for CO2 Geostorage, Acc. Chem. Res., 50(5), 1134-1142 (2017)
9. F. Alnili, A. Al-Yaseri, H. Roshan, T. Rahman, etc., Carbon dioxide/brine wettability of porous sandstone versus solid quartz: An experimental and theoretical investigation, J. Coll. Interf. Sci., 524, 188-194 (2018)
10. F. Haeri, D. Tapriyal, S. Sanguinito, F. Shi, S. Fuchs, etc., CO2–Brine Contact Angle Measurements on Navajo, Nugget, Bentheimer, Bandera Brown, Berea, and Mt. Simon Sandstones, Eng. & Fuels, 34(5), 6085-6100 (2020)
11. R. Juanes, EJ Spiteri, FM Orr, MJ Blunt, Impact of relative permeability hysteresis on geological CO2 storage, Water Resour. Res., 42, W12418 (2006)

12. EJ Spiteri, R. Juanes, MJ Blunt, FM Orr, A New Model of Trapping and Relative Permeability Hysteresis for All Wettability Characteristics, SPE J., 13(3), 277-288 (2008)
13. S. Krevor, R. Pini, L. Zuo, SM Benson, Relative permeability and trapping of CO2 and water in sandstone rocks at reservoir conditions, Water Resour. Res., 48, W02532 (2012)
14. C. Reynolds, M. Blunt, S. Krevor, The impact of CO2-brine interfacial tension on the relative permeability of the CO2-brine-sandstone system at reservoir conditions, SCA2013-033 presented at the International Symposium of the Society of Core Analysts, Napa Valley, USA, 16-19 September 2013
15. NM Burnside, M. Naylor, Review and implications of relative permeability of CO2/brine systems and residual trapping of CO2, Int. J. Greenh. Gas Control, 23, 1-11 (2014)
16. S. Krevor, C. Reynolds, A. Al-Menhali, B. Niu, The impact of reservoir conditions on multiphase flow in the CO2-brine system in permeable sandstone, SCA2015-019 presented at the International Symposium of the Society of Core Analysts, St. John's, Canada, 16-21 August 2015
17. X. Chen, S. Gao, A. Kianinejad, DA Dicarlo, Steady-state supercritical CO2 and brine relative permeability in Berea sandstone at different temperature and pressure conditions, Water Resour. Res., 53(7), 6312-6321 (2017)
18. J. Moore, P. Holcomb, D. Crandall, S. King, etc., Rapid determination of supercritical CO2 and brine relative permeability using an unsteady-state flow method, Adv. in Water Resour., 153, 103953 (2021)
19. Y. Yuan, K. Dugan, P. Krishnamurthy, S. Morgan, etc., Simulation of large-scale geological carbon sequestration in the Gulf of Mexico using fully coupled flow and geomechanics, Paper presented at the SPE/AAPG/SEG CCUS Workshop, Houston, USA, 25-27 April 2023
20. A. Lee, D. Tapriyal, D. Crandal, A. Goodman, etc, Caprock Wettability Under CO2 Geostorage Conditions, Paper presented at the SPE/AAPG/SEG CCUS Workshop, Houston, USA, 25-27 April 2023
21. S. Morgan, AK Singh, K. Kohli, A. Pal, etc., Geomechanical Simulation Case Study of CO2 Injection in the LaBarge Field Wyoming, Paper presented at the SPE/AAPG/SEG CCUS Workshop, Houston, USA, 25-27 April 2023
22. L. Lun, B. Gao, P. Krishnamurthy, K. Kohli, RC. Wattenbarger, Developing consistent relative permeability and capillary pressure models for reservoir simulation of CCS projects, SPE-216722-MS presented at the Abu Dhabi International Petroleum Exhibition and Conference, Abu Dhabi, UAE, October 2023
23. P. Likanapaisal, L. Lun, P. Krishnamurthy, K. Kohli, Range of Carbon Storage Performance in Saline Aquifer, a Simulation Sensitivity Study, Poster presented at the SPE/AAPG/SEG CCUS Workshop, Houston, USA, 25-27 April 2023
24. EM Braun, RJ Blackwell, A Steady-State Technique for Measuring Oil-Water Relative Permeability Curves at Reservoir Conditions, SPE-10155-MS presented at the SPE Annual Technical Conference and Exhibition, San Antonio, Texas, October 1981
25. J. Kestin, H. Ezzat Halifa, RJ Correia, Journal of Physical and Chemical Reference Data **10**, 71 (1981)
26. https://www.nist.gov/
27. AL Chen, AC Wood, Rate Effects on Water-Oil Relative Permeability. SCA2001-19 presented at the International Symposium of the Society of Core Analysts, Edinburgh, UK, 17–19 September 2001.
28. R Gupta, DR Maloney, Intercept Method—A Novel Technique To Correct Steady-State Relative Permeability Data for Capillary End Effects, SPE Res Eval & Eng 19 (02): 316–330 (2016)
29. CS Land, Comparison of Calculated with Experimental Imbibition Relative Permeability, SPEJ, 11(4), 419-425 (1971)
30. Killough, J.E., Reservoir Simulation With History-Dependent Saturation Functions, SPE J. 16 (01): 37–48 (1976)
31. R. Wiebe, VL Gaddy, Vapor Phase Composition of Carbon Dioxide-Water Mixtures at Various Temperatures and at Pressures to 700 Atmospheres, J. Am. Chem. Soc., 63(2), 475-477 (1941)